SIMULATION AND PERFORMANCE EVALUATION OF OWC DEVICE OPERATING IN COASTAL REGIONS

BELIBASSAKIS K.[1,*], MAGKOURIS A.[1] and RUSU E.[2]

1 School of Naval Architecture & Marine Engineering, National Technical University of Athens, Heroon Polytechniou 9, 15780 Zografou, Greece

2 Department of Mechanical Engineering, University Dunarea de Jos of Galati, Strada Domneasca 47, 800008 Galati, Romania

*corresponding author:
e-mail: kbel@fluid.mech.ntua.gr

Abstract: Wave energy converters are constantly being deployed in nearshore and coastal areas characterized by increased wave potential. The performance of the devices installed in the nearshore and coastal environment, where the sea bottom terrain may present significant variations, can be evaluated by formulating and solving interaction problems that involve water waves, structures and the seafloor. In this work a novel Boundary Element Method (BEM) is developed and applied to the investigation of a simplified Oscillating Water Column (OWC) system in the two-dimensional space, taking into account the interaction of the incident wave field with the bottom topography, in the context of the linear wave theory for normally incident waves. Numerical results that highlight the effect of seabed inhomogeneities on the hydrodynamic performance of OWC devices are presented, in combination with other parameters that determine the device's performance, like the structure's dimensions and power take off system. Finally, results related to the flow field developed during the operation of the device are presented and discussed.

Keywords: Oscillating Water Column, wave energy, BEM

1. Introduction

Our planet's oceans contain vast amounts of energy that modern technology has not yet been able to harness and use effectively, in contrast to other renewables that are currently contributing at a significant scale to the global energy grid. Among many concepts and devices that have been proposed and developed for the exploitation of wave energy, the OWC is one of the most commercially mature, as a result of extensive studies, both in theory and in practice, by means of prototype devices' deployment. An OWC essentially comprises of a solid chamber enclosing an air mass. As the lower part of chamber is open to sea water, at a certain distance from Still Water Level (SWL), the water surface elevation in the chamber oscillates due to incident wave fields (see Fig. 1) acting like a piston. These fluctuations of the water surface elevation successively compress and decompress the air mass, which is then channelled through a Power Take Off System, which usually involves a bidirectional turbine and an electric power generator.

In the context of linear wave theory, the velocity of the flow field in a domain D, around the device, is expressed by the gradient of the (scalar) velocity potential function Φ. Harmonic time dependence in the form of $\exp(-i\omega t)$ is considered, where ω is the frequency of the incident wave field, which coincides with the device's operation frequency, due to linearity. This allows for the numerical model to be developed in the frequency domain, by defining the complex wave potential function φ, so that:

$$\Phi(\mathbf{x};t) = \mathrm{Re}\left\{\varphi(\mathbf{x})\exp(-i\omega t)\right\},\quad \mathbf{x}=(x,z)\in D\,. \qquad (1)$$

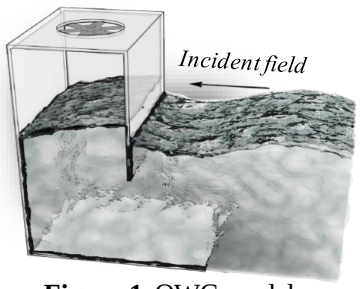

Figure 1. OWC model

2. Definition of the Boundary Conditions

Let $D=\{0\le x,\ -h(x)\le z\le 0\}$ denote a semi-infinite geometrical domain, occupied by seawater, with the OWC configuration starting at the horizontal position $x=0$ and $z=-h(x)$ denoting the seabed profile, where h is the depth, as shown in Fig. 2. A low-order BEM is developed by Belibassakis et al (2020) to simulate operation in the frequency domain. The numerical method requires a closed boundary geometry, which is achieved by introducing a vertical boundary of D at the horizontal position $x=x_b$, serving as an incidence-radiation interface. D is therefore enclosed by the curve $\partial D=\bigcup_{i=1}^{8}\partial D_i$, with ∂D_1 and ∂D_5 being the outer and inner free surfaces of the water respectively and $\partial D_7, \partial D_8$ denoting the seabed and the radiation interface. Finally, ∂D_i, $i=2,3,4,6$ are the lines that shape the walls of the chamber. The linearized Free-Surface Boundary Condition (FSBC) applies to the free surface out of the OWC's

chamber, which formulated with respect to the complex potential φ, for harmonic time dependence is:

$$\frac{\partial\varphi(\mathbf{x})}{\partial n}-\frac{\omega^2}{g}\varphi(\mathbf{x})=0,\ \mathbf{x}\in\partial D_1\ , \tag{2}$$

where g is the gravitational acceleration. Impermeability Boundary Conditions apply to all rigid walls as well as to the seabed, imposing vanishing of the velocity normal to these boundary sections (see Fig.2):

$$\frac{\partial\varphi(\mathbf{x})}{\partial n}=0,\ \mathbf{x}\in\left(\bigcup_{i=2}^{4}\partial D_i\cup\bigcup_{i=6}^{7}\partial D_i\right)\ . \tag{3}$$

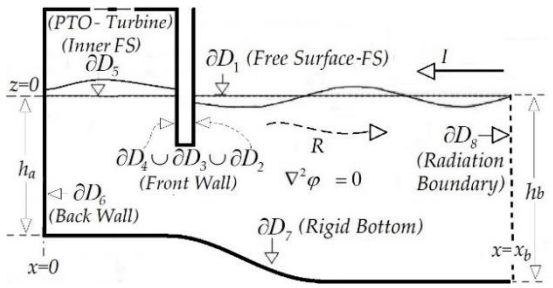

Figure 2. 2D OWC model and boundary sections

The Radiation Condition that applies on the interface ∂D_8 derives from appropriate formulation of the general representation of the complex velocity potential, that describes monochromatic wave propagation in a 2D semi-infinite strip of constant depth h, as follows:

$$\varphi(\mathbf{x})=\left[A_0^{+}\exp(ik_0x)+A_0^{-}\exp(-ik_0x)\right]Z_0(z)+ \\ +\sum_{n=1}^{\infty}\left[A_n\exp(-ik_nx)\right]Z_n(z),\ \ x\geq x_b,-h(x)<z<0, \tag{4}$$

where A_0^{-},A_0^{+} are the amplitudes of the incident and the reflected propagating mode, respectively while A_n are the evanecent-mode coefficients. The functions $\{Z_n(z)\}_{n=0}^{\infty}$ are defined as $Z_n(z)=\cosh\left[k_n(z+h)\right]/\cosh(k_nh)$ and are obtained as the solutions of Sturm Liouville problem (Coddington & Levinson, 1972), to which Laplace's equation is reduced in the constant depth strip $\{-h<z<0,x\geq x_b\}$, and the corresponding eigenvalues k_0 and $\{k_n\}_{n=1}^{\infty}$ are respectively obtained as the real root and the imaginary roots of the dispersion relation:

$$\omega^2=kg\cdot\tanh(kh)\ . \tag{5}$$

Further assuming that the evanecent modes are negligible at $x=x_b$ we obtain:

$$\varphi(\mathbf{x})=Q^{-1}\left[R\exp(ik_0x)+\exp(-ik_0x)\right]Z_0(z),x\geq x_b, \tag{6}$$

where $Q=-igH/2\omega$, with H denoting the incident waveheight. The latter quantity is used to normalize the potential and assume an incident field with unit-amplitude $(A_0^{-}=1)$. By projection the two members of Eq.(6) on the orthonormal basis spanned by the eigenmodes $\{Z_n(z)\}_{n=0}^{\infty}$, we obtain the following expression for the reflection coefficient $R=A_0^{+}$ (see also Magkouris et al, 2020):

$$R=\|Z_0\|^{-2}\,\mathrm{e}^{-ik_0x_b}\int_{z=-h}^{z=0}\varphi(x_b,z)\cdot Z_0(z)\,dz-\mathrm{e}^{-2ik_0x_b}\ . \tag{7}$$

Subsequently, by differentiation of Eq.(5) with respect to x and substitution of R from Eq.(7) we obtain the following form for the Radiation Condition:

$$\frac{\partial\varphi}{\partial x}-\frac{\int_{z=-h}^{z=0}\varphi(x_b,z)\cdot Z_0(z)\,dz}{\|Z_0(z)\|^2}Z_0(z)= \\ =-2ik_0\exp(-ik_0x_b)Z_0(z),\mathbf{x}\in\partial D_8\ . \tag{8}$$

Definition of the Boundary Condition that applies on the water's inner free surface requires calculating the time dependent pressure of the entrapped air mass, for which harmonic dependence is also considered. The analysis is simplified by assuming isentropic compression and decompression during the device's operation (Malara & Arena, 2013) and therefore the air density ρ and pressure P_c are related by the heat capacity ratio γ as follows:

$$\frac{\dot\rho(t)}{\rho(t)}=\frac{1}{\gamma}\frac{\dot P_c(t)}{P_c(t)}\ . \tag{9}$$

The entrapped air volume and its rate of change are:

$$V(t)=bL\left[h_c-A(t)\right],\ \dot V(t)=-bL\dot A(t) \tag{10}$$

with b,h_c respectively denoting the horizontal and vertical dimension of the chamber, L being the length of the configuration in the transverse direction and $A(t)$ being the time dependent, mean free surface elevation.

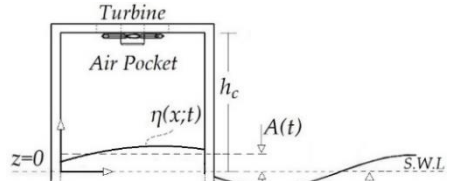

Figure 3. Air pocket and dimensions notation

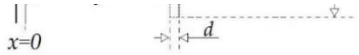

The air mass in the chamber is equal $M(t)=\rho(t)V(t)$. Hence, by differentiating with respect to time and substituting the expressions for ρ and $\dot\rho$:

$$\dot M(t)=\left[\frac{1}{\gamma}\frac{\dot P_c(t)}{P_c(t)}-\frac{\dot A(t)}{h_c-A(t)}\right]M(t)\ . \tag{11}$$

The air mass rate $\dot m(t)$, flowing out of the chamber, equals to $-\dot M(t)$. Furthermore, it is assumed that the pressure is equal to the sum $P_c(t)=P_0+\delta P_c(t)$, where P_0 is the atmospheric pressure. Thus $\dot P_c(t)=\delta\dot P_c(t)$. From the above we obtain that:

$$\delta\dot P_c(t)=-\frac{\gamma\left[P_0+\delta P_c(t)\right]}{h_c-A(t)}\left\{\frac{\dot m(t)}{bL\rho_0}\left[\frac{P_0}{P_c(t)}\right]^{1/\gamma}-\dot A(t)\right\}\ . \tag{12}$$

The term to the power of $(1/\gamma)$ is excluded from the analysis as being approximately equal to 1, assuming pressure fluctuations of small amplitude $(\|\delta P_c\|=P_0)$. Eq. (11) is then put to the frequency domain by using the

complex amplitudes $\tilde{p}, \tilde{m}$ and $\tilde{A}$ for the time-harmonic quantities $\delta P_c(t), \dot{m}(t)$ and $A(t)$ as follows:

$$i\omega\tilde{p} = \frac{\gamma\tilde{p}}{h_c - \tilde{A}}\left(\frac{-i\omega\tilde{m}}{bL\rho_0} + i\omega\tilde{A}\right) + \frac{\gamma P_0}{h_c - \tilde{A}}\left(\frac{-i\omega\tilde{m}}{bL\rho_0} + i\omega\tilde{A}\right), \quad (13)$$

where ρ_0 is the atmospheric air density. The mean surface elevation is evaluated as:

$$\tilde{A} = \tilde{\eta}_{average} = -\frac{1}{i\omega b}\int_0^b \frac{\partial\tilde{\varphi}(x,0)}{\partial z}dx \quad . \quad (14)$$

A linear model is next introduced which relates the air mass flow rate $\dot{m}(t) = -i\omega\tilde{m}$ to the air pressure difference $\left[P_c(t) - P_0\right]$, so that $-i\omega\tilde{m} = \lambda_T\tilde{p}$, where λ_T denotes the parameter of the turbine. Using the later in Eq. (12) and keeping only linear terms we get:

$$\tilde{p} = i\omega A P_0\left(\frac{i\omega h_c}{\gamma} - \frac{\lambda_T P_0}{bL\rho_0}\right)^{-1}. \quad (15)$$

Furthermore, from Bernoulli's equation the complex amplitude of pressure equals $\tilde{p} = i\omega\rho\tilde{\varphi}(x,0) - \rho g\tilde{\eta}(x)$ on the inner free surface. Hence by using the latter in Eq. (14):

$$\frac{\partial\tilde{\varphi}(x,0)}{\partial n} - \frac{\omega^2}{g}\tilde{\varphi} - C(\omega)\int_0^b \frac{\partial\tilde{\varphi}(x,0)}{\partial z}dx = 0, \ \mathbf{x}\in\partial D_5 \ , \quad (16)$$

Where the frequency-dependent parameter C, which carries information regarding the geometry and the turbine's characteristics, is equal to:

$$C(\omega) = \frac{i\omega P_0}{\rho g}\left(\frac{i\omega h_c}{\gamma} - \frac{\lambda_T P_0}{bL\rho_0}\right)^{-1}. \quad (17)$$

More details concerning the above formulation are found in Belibassakis et al. (2020).

3. Numerical Formulation

A low order BEM is developed for simulating the OWC's operation. All sections of ∂D are approximated by a number of linear elements, each carrying a simple source-sink distribution of constant strength σ_j. Let M_i denote the number of boundary elements distributed across ∂D_i and M be the total number of elements $\left(M = M_1 + M_2 + ... + M_8\right)$. Then, the solution for a given frequency, which is the vector $\sigma_j, j\in[1,2,...,M]$, is obtained via the solution of a linear system of the form:

$$\sum_{j=1}^{M} A_{kj}\sigma_j = b_k, \ \ k = 1,2,...,M \ . \quad (18)$$

Each of the above algebraic equations ensures the satisfaction of the appropriate boundary condition - by the summation of induced potential and velocities - at a collocation point, which is chosen to coincide with the midpoint of the element k. The influence matrix A_{jk}, $j,k = 1,2,...,M$, is defined so that its lines form a discretized version of the appropriate BC for each element, with the aid of the induced potential and velocity matrices φ_{jk} and $\mathbf{U}_{jk}$ $j,k = 1,2,...,M$, where each element respectively contains the potential and velocity induced at the k-collocation point due to a unit source distribution along the j-element. In particular, the algebraic equations that impose implementation of the impermeability BC on the sections of ∂D numbered as 2,3,4,6 and 7, are formulated in discrete form as follows:

$$\sum_{j=1}^{M}\sigma_j\left(\mathbf{n}_k\mathbf{U}_{kj}\right) = 0, \mathbf{x}_k \in \left\{\bigcup_{i=2}^{7}\partial D_i \ \Big| \left[\mathbf{x}_k \in \left(\partial D_5\right)\right]\right\} \ , \quad (19)$$

with $\mathbf{n}_k$ being the unit vector normal to the k-element, directed outwards, with respect to the domain. Moreover, the FSBC on ∂D_1 becomes:

$$\sum_{j=1}^{M}\sigma_j\left(\mathbf{n}_k\mathbf{U}_{kj} - \frac{\omega^2}{g}\varphi_{kj}\right) = 0, \mathbf{x}_k \in \left\{\partial D_1\right\} \ . \quad (20)$$

The integral involved in Eq. (7) is numerically evaluated using the trapezoidal rule, and thus the radiation condition is implemented on ∂D_8 as follows:

$$\sum_{j=1}^{M}\left\{(\mathbf{n}_k\mathbf{U}_{kj}) - ik_0\left[\sum_{a=M-M_8+1}^{M}\sigma_j\varphi_{\alpha j}\delta z_8 Z_0^{(b)}(z_a)\right]Z_0^{(b)}(z_k)\right\} =$$
$$= -2ik_0\exp(-ik_0x_b)Z_0(z_k), \quad \mathbf{x}_k\in\partial D_8 \ , \quad (21)$$

with $\delta z_8 = h_b/M_8$. Similarly, the BC on the free surface inside the chamber becomes:

$$\sum_{j=1}^{M}\sigma_j\left[\mathbf{n}_k\mathbf{U}_{kj} - \frac{\omega^2}{g}\varphi_{kj} - \frac{1}{b}C(\omega)\sum_{\alpha=1+M_B}^{M_B+M_5}\delta x_5\mathbf{n}_a\mathbf{U}_{aj}\right] = 0,$$
$$\mathbf{x}_k\in\partial D_8 \text{ , with } M_B = M_1 + M_2 + M_3 + M_4 \ , \quad (22)$$

and $\delta x_5 = b/M_5$. Finally, given that the complex wave potential has been normalized with respect to the incident wave height H_I and the reflected wave is of height $H_R = |R|H_I$, the hydrodynamic performance of the configuration is obtained by:

$$\eta_{OWC} = \frac{P_{out}}{P_{in}} = \left(1 - |R|^2\right) \quad , \quad (23)$$

with the Reflection Coefficient R calculated by Eq.(6) as:

$$R = \frac{\sum_{a=M-M_8+1}^{M}\left(\sum_{j=1}^{M}\sigma_j\varphi_{aj}\delta z_8 Z_0(z_a)\right)}{\|Z_0\|^2\exp(ik_0x_b)} - \exp(-2ik_0x_b) \ . \quad (24)$$

4. Numerical Results

The present model allows for the evaluation of an OWC hydrodynamic performance taking into account the interaction of the flow field with arbitrary seabed profile. As an example, we consider a domain with depth varying from $h_a = 10m$ at $x = 0$ to $h_b = 20m$ at $x_b = 200m$ described by the function:

$$h(x) = \frac{1}{2}(h_a + h_b) - \frac{1}{2}(h_a + h_b)\tanh\left[S_h\left(x - \frac{x_b}{2}\right)\right] + \delta h(x), \quad (25)$$

with the parameter S_h, that is used to control maximum slope, set to $S_h = 5\cdot10^{-2}$, and the function $\delta h(x)$, that models additional seabed irregularities defined as:

$$\delta h(x) = 5\cdot\sin\left[0.1\left(x - \frac{x_b}{2}\right)\right]\cdot\exp\left[15\cdot10^{-4}\left(x - \frac{x_b}{2}\right)^2\right]. \quad (26)$$

We further assume that the chamber's dimensions are $b = 3m$, $h_c = 6m$ and the configuration extends in the transverse direction $L = 200m$. The front wall draft is $D = 4m$ and is of thickness $d = 0.7m$. Finally, the non-dimensional parameter $\hat{\lambda}_T$ of the turbine near the considered operation point is

$$\hat{\lambda}_T = \lambda_T \left(g / b^3 \right)^{0.5} = 1.5 \ . \quad (27)$$

The resulting depth profile and the achieved hydrodynamic performance are illustrated in Fig 4. It can be observed that low-frequency waves, characterized by larger wavelengths, strongly interact with the seabed, leading to variations to the achieved power output, while in the case of higher frequencies the depth profile is of no importance. As shown in previous work (Belibassakis et al 2020), the performance of OWC configurations with low natural frequencies is more dependent on the local topography. This is also noticeable in the alternative performance curve of Fig. 4(b), for a similar configuration with different draft and width of the front wall.

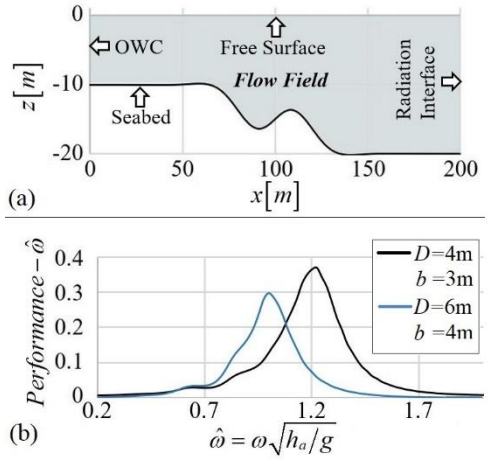

Figure 4. Domain of operation (a) and performance as a function of the non-dimensional frequency (b)

By defining a 2D grid spanning the entire 2D space, the distribution of the wave potential across the whole flow field can be obtained by the superposition of the potential induced from each element to the grid's points. Subsequently, the flow field can be represented in the time domain, calculated according to Eq. (1), as illustrated in Fig. 5 for the aforementioned dimensions and parameters, near the device, for an incident wave field of frequency $\omega = 1.3 rad/s$. One can graphically verify the implementation of impermeability conditions on all solid boundaries of the flow filed, as they are normally intersected by the equipotential lines. This leads the velocity field, which is defined as the potential function's gradient, to be tangent to these boundary sections, as the normal velocity is zero.

5. Concluding Remarks

In this work, a BEM is developed and applied to investigate OWC responses and performance under the assumptions of the linear wave theory in two dimensions. Although the present simplified model does not account for three-dimensional and non-linear phenomena it still

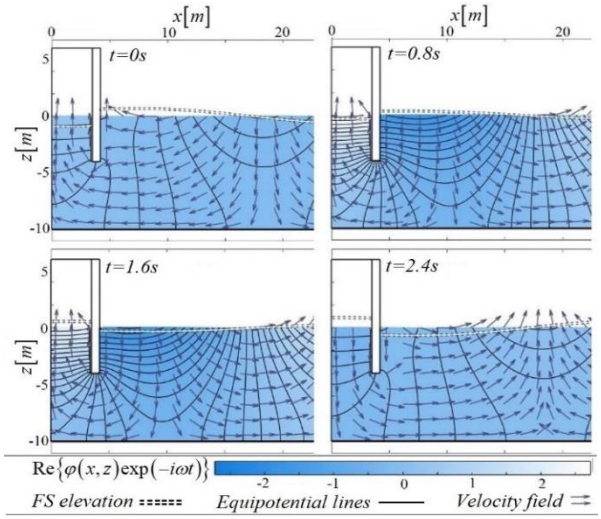

provides useful information of the considered system's dynamics, especially regarding the interaction of the wave fields with the seabed profile and the OWC configuration.

Figure 5. Representation of the flow field in the time domain

The present method is of relatively low computational cost and can be applied to investigate any OWC geometry, and in particular configurations that have been proposed to increase its performance like the U-OWC; see e.g. (Boccotti, 2003). Furthermore, the present model can be systematically applied in conjunction with climatological wave data of a nearshore/coastal region in order to derive long-term predictions and monthly variations of power output, as presented by Belibassakis et al (2020) in a region of the Black Sea, where previous studies (Rusu, 2019) had indicated relatively higher wave potential.

Acknowledgements

This work has been supported by the research project DREAM funded by the Romanian Executive Agency for Higher Education, Research, Development and Innovation Funding–UEFISCDI, grant number PNIII-P4-ID-PCE-2020-0008.

References

Belibassakis, K., Magkouris, A., & Rusu, E. (2020). A BEM for the Hydrodynamic Analysis of Oscillating Water Column Systems in Variable Bathymetry. MDPI Energies 13, 3403.

Boccotti, P. (2003). On a new wave energy absorber. Ocean Engineering 30(9), 1191-1200.

Coddington, E., & Levinson, N. (1972). Theory of Ordinary Differential Equations. New Delhi, India: McGraw Hill Publishing Co. Ltd.

Magkouris, A., Bonovas, M., & Belibassakis, K. (2020). Hydrodynamic Analysis of Surge-Type Wave Energy Devices in Variable Bathymetry by Means of BEM. MDPI *Fluids* 5(2), 99.

Malara, G., & Arena, F. (2013). U-Oscillating Water Column in random waves: Modelling and Performances. 32nd Intern. Conf. on Ocean, Offshore and Arctic Engineering. Nantes, France.

Rusu, L. (2019). The wave and wind power potential in the western Black Sea. Renewable Energy139(C), 11.